

Supplementary Material to

Broadband Ground Motion Synthesis via Generative Adversarial Neural Operators: Development and Validation

Shi Y., Lavrentiadis G., Asimaki D., Ross Z.E., and Azizzadenesheli K.

February 8, 2024

As an illustrative example, Fig S1. compares the time history and Fourier Amplitude Spectrum acceleration, velocity, and displacement of a M_w 6.9, $R_{rup} = 23\text{km}$ event recorded at station ISKH02 of the Kik-Net strong motion network with $V_{s30} = 721\text{m/s}$. In the figure, the acceleration time series are rich in high frequencies and attain constant Fourier spectral content at frequencies larger than $\sim 5\text{Hz}$. The opposite is true for displacement time series, their energy content decays for frequencies higher than 0.1Hz . Spanning a much broader frequency range of spectral amplitudes from ~ 0.1 to 10Hz , the velocity time series provided the optimal balance of input frequency content to train cGM-GANO in the broadband frequency range $0.1 \sim 30\text{Hz}$.

Fig S2 shows the fault location (indicated by the black line) and the corresponding station positions (depicted as red dots) used in the BBP simulation. The yellow star on the fault represents the hypocenter.

Fig S3 compares acceleration time history and Fourier amplitude spectrum of BBP and cGm-GANO generated ground motions for both strike-slip and reverse scenarios under $M_w = 7.0$, $R_{rup} = 10\text{ km}$. In this figure, cGm-GANO captures the envelope of the BBP waveforms in the time domain. In the frequency domain.

Fig S4 presents the inter-frequency correlation of the cGM-GANO synthetically generated ground motions based on the BBP dataset.

Fig S5 shows the residual results of Fig 10 using only the validation Kik-Net dataset; that is, the subset not included in the training of cGm-GANO. The negligible differences between Fig 10 and S5 indicate no overfitting on the training dataset.

Fig S6 and S7 compare the velocity and displacement time histories between data and synthetic ground motions from cGM-GANO for the same scenarios shown in Figure 8.

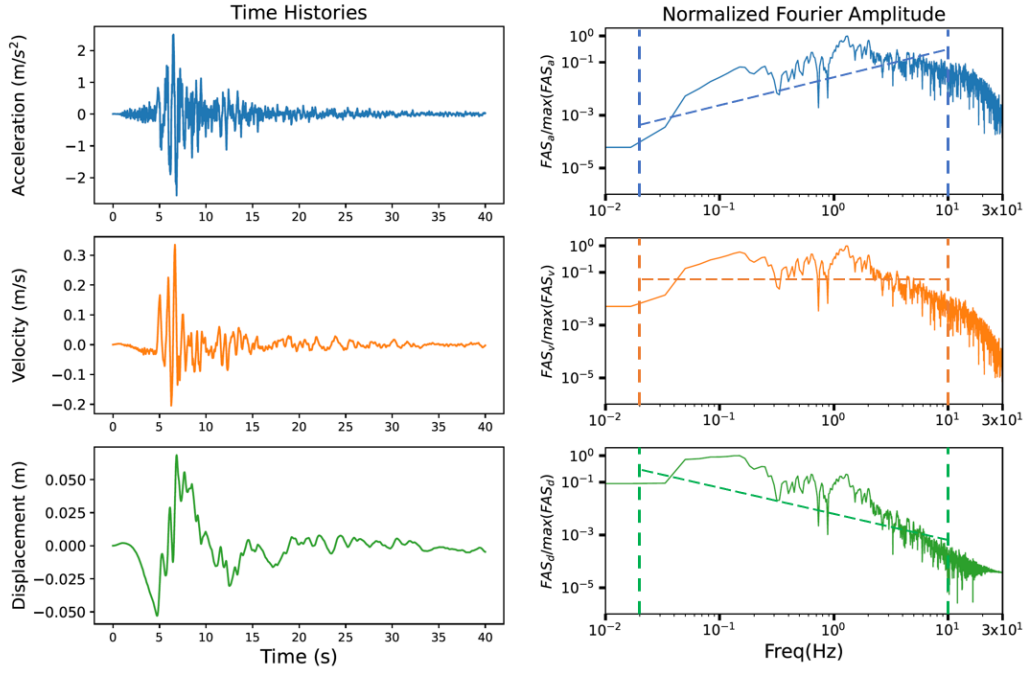


Figure 1: Example of frequency content shift between acceleration, velocity, and displacement time series, depicted in the time and frequency domain. Example time series corresponds to event id ISKH020703250942 with $M_w = 6.9$ and $R_{rup} = 23km$ from the Kik-net dataset. The left-hand panels show the acceleration, velocity, and displacement time series from top to bottom, while the right-hand panels show the corresponding normalized frequency amplitude spectra. Each spectrum is normalized by its maximum amplitude. The dash lines show the FAS trend in 0.02Hz \sim 10Hz frequency range.

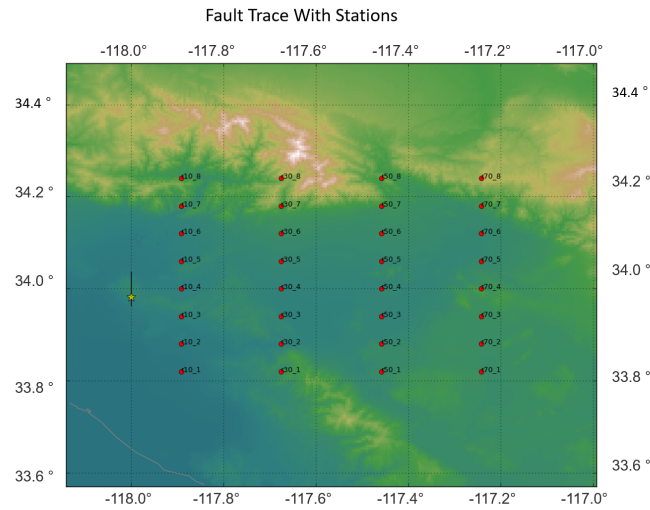
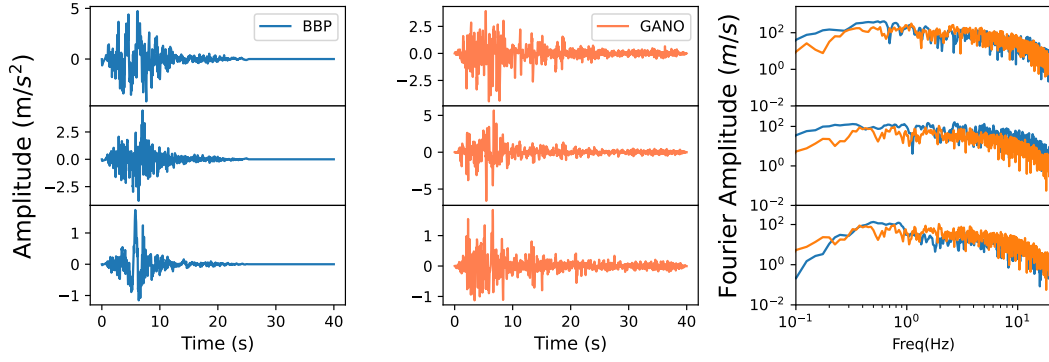


Figure 2: An example of the location of the fault (black line) and stations (red dots) used in BBP simulation.

(a)

M 7.0, 10 km, Strike Slip



(b)

M 7.0, 10 km, Reverse

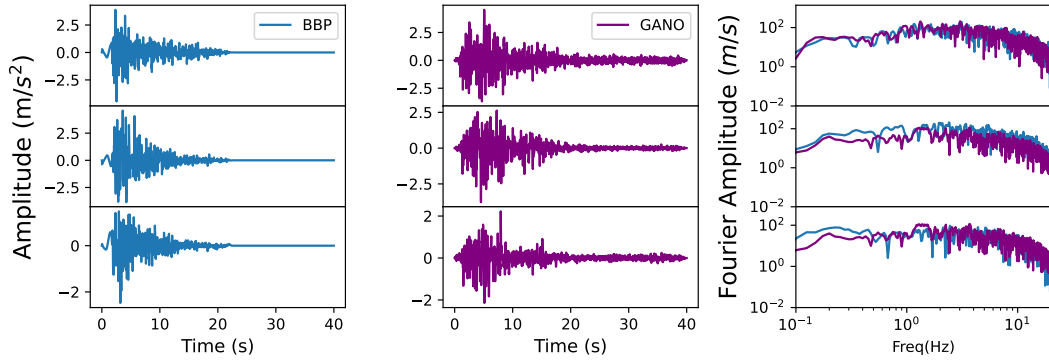


Figure 3: Time-domain and frequency-domain waveforms comparisons of BBP and GANO generated ground motions. Subfigure (a) corresponds to a three-component waveform comparison for $M_w = 7$, $R_{rup} = 10\text{ km}$, and strike-slip style of faulting. Subfigure (b) corresponds to a three-component waveform comparison for $M_w = 7$, $R_{rup} = 10\text{ km}$, and reverse style of faulting.

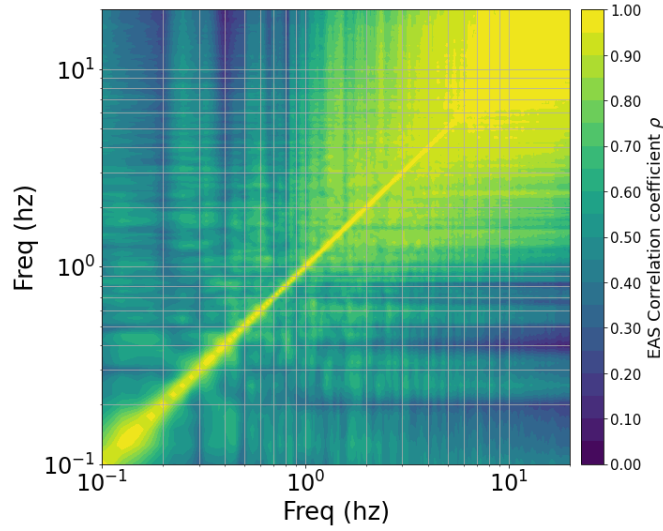


Figure 4: Inter-frequency correlation of synthetically generated ground motions through cGM-GANO based on the BBP training dataset.

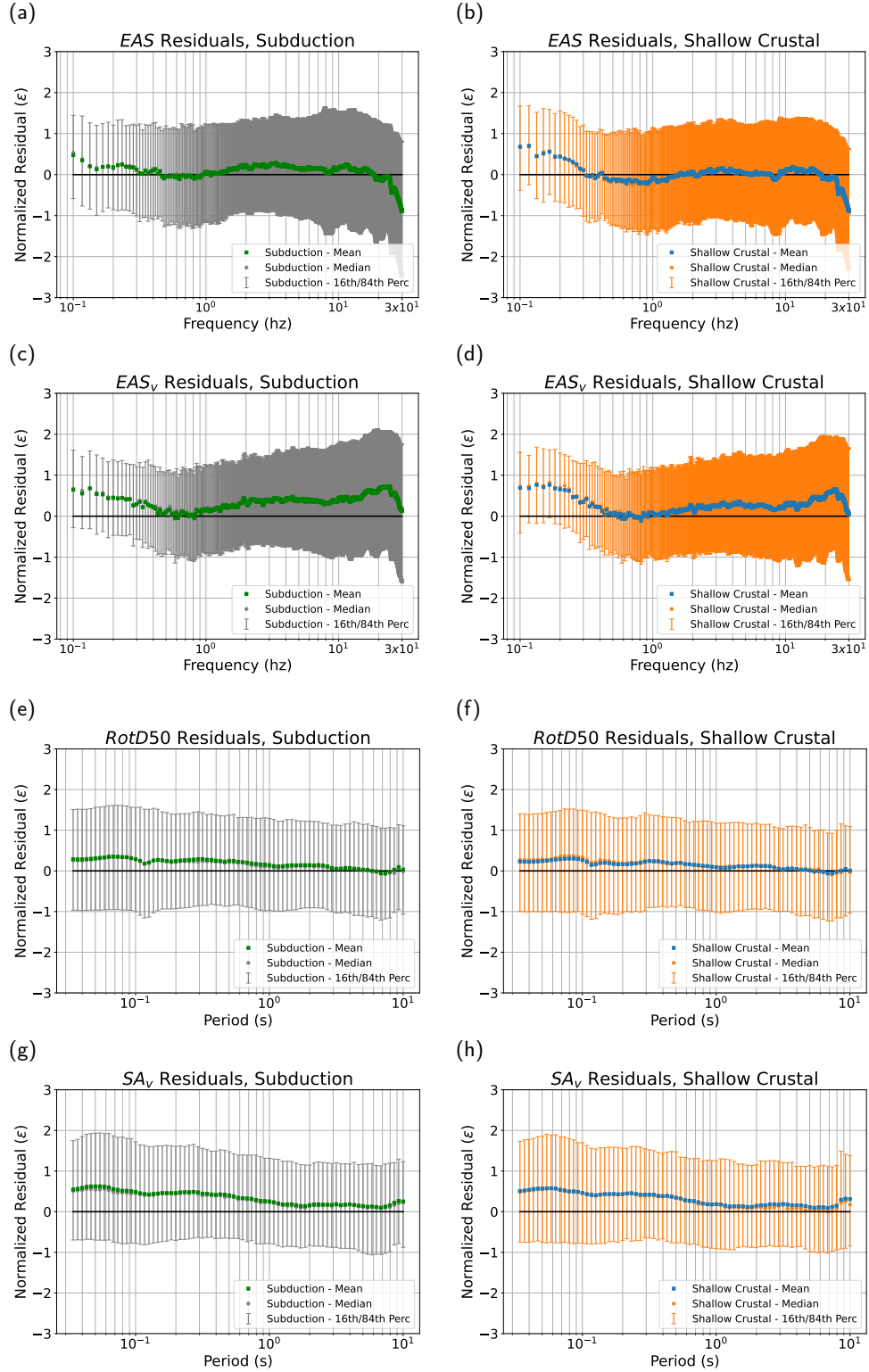
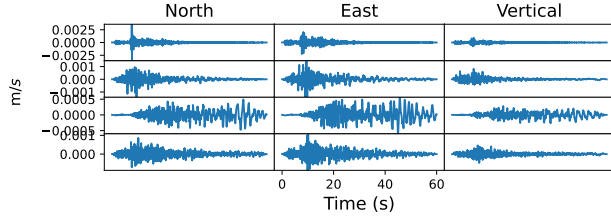
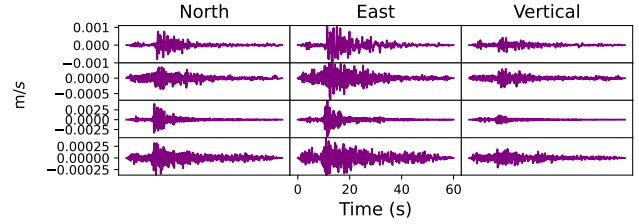


Figure 5: Residual plots of the kik-net trained model based on the validation kik-net dataset (10 % of the total kik-net dataset) . Subfigures (a) and (b) show the horizontal EAS residuals for subduction and shallow crustal events, respectively. Subfigures (c) and (d) show the vertical EAS residuals for subduction and shallow crustal events, respectively. Subfigures (e) and (f) show the horizontal RotD50 PSA residuals for subduction and shallow crustal events, respectively. Subfigures (g) and (h) show the vertical PSA residuals for subduction and shallow crustal events, respectively.

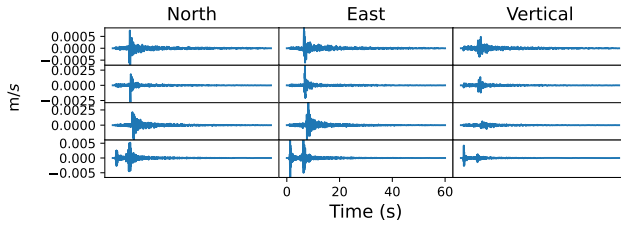
(a) Observation: M 4.5, 50 km, 300 m/s, Shallow Crustal, Velocity



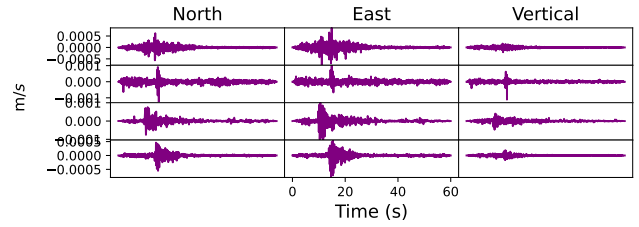
(b) GANO: M 4.5, 50 km, 300 m/s, Shallow Crustal, Velocity



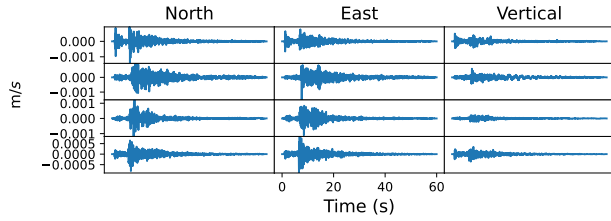
(c) Observation: M 4.5, 50 km, 700 m/s, Subduction, Velocity



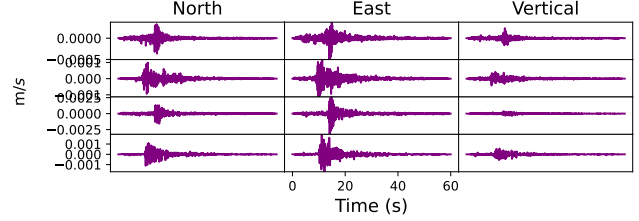
(d) GANO: M 4.5, 50 km, 700 m/s, Subduction, Velocity



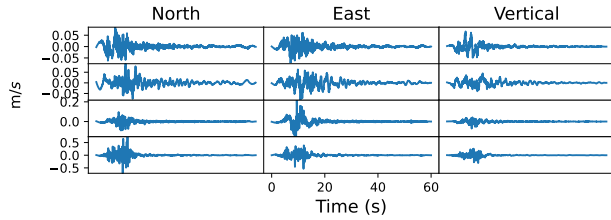
(e) Observation: M 4.5, 50 km, 700 m/s, Shallow Crustal, Velocity



(f) GANO: M 4.5, 50 km, 700 m/s, Shallow Crustal, Velocity



(g) Observation: M 7.2, 20 km, 500 m/s, Shallow Crustal, Velocity



(h) GANO: M 7.2, 20 km, 500 m/s, Shallow Crustal, Velocity

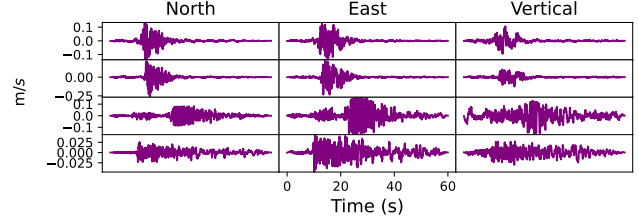
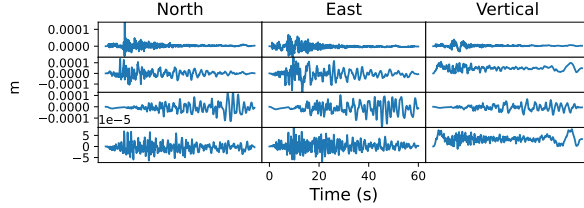


Figure 6: Velocity waveforms comparisons between data and synthetic ground motions from cGM-GANO trained on the Kik-net dataset, unit in m/s .

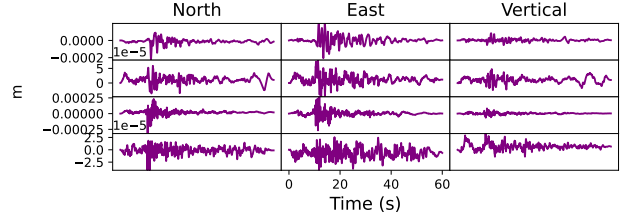
(a)

Observation: M 4.5, 50 km, 300 m/s, Shallow Crustal, Displacement



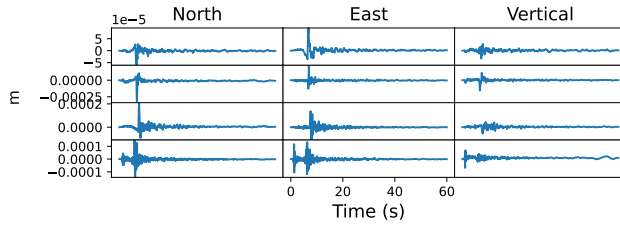
(b)

GANO: M 4.5, 50 km, 300 m/s, Shallow Crustal, Displacement



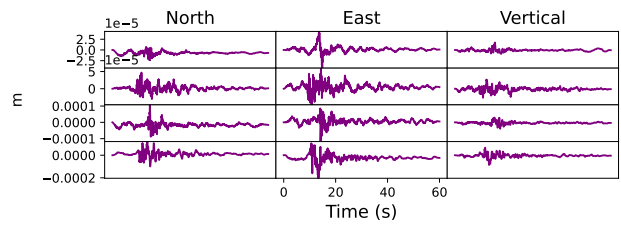
(c)

Observation: M 4.5, 50 km, 700 m/s, Subduction, Displacement



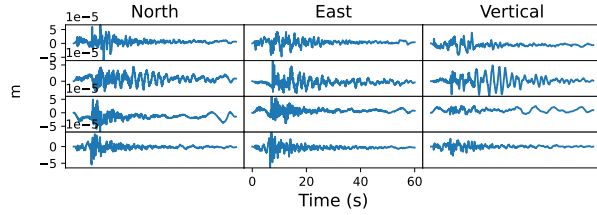
(d)

GANO: M 4.5, 50 km, 700 m/s, Shallow Crustal, Displacement



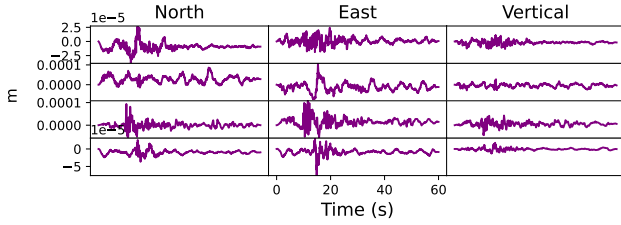
(e)

Observation: M 4.5, 50 km, 700 m/s, Shallow Crustal, Displacement



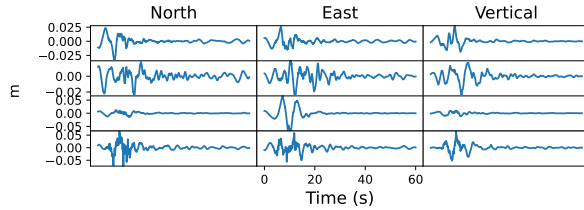
(f)

GANO: M 4.5, 50 km, 700 m/s, Subduction, Displacement



(g)

Observation: M 7.2, 20 km, 500 m/s, Shallow Crustal, Displacement



(h)

GANO: M 7.2, 20 km, 500 m/s, Shallow Crustal, Displacement

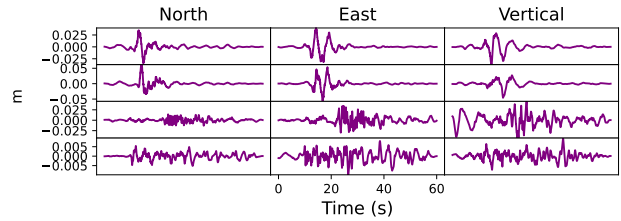


Figure 7: Displacement waveforms comparisons between data and synthetic ground motions from cGM-GANO trained on the Kik-net dataset, unit in m .